Available online at www.sciencedirect.com
SCIENCE DIRECT®
Applied Radiation and Isotopes 62 (2005) 711–720
Applied Radiation and Isotopes
www.elsevier.com/locate/apradiso

# Labelling of manganese-based magnetic resonance imaging (MRI) contrast agents with the positron emitter $^{51}$Mn, as exemplified by manganese-tetraphenyl-porphin-sulfonate ($MnTPPS_4$)

A.T.J. Klein[1], F. Rösch[2], H.H. Coenen, S.M. Qaim*

*Institut für Nuklearchemie, Forschungszentrum Jülich GmbH, D-52425 Jülich, Germany*

Received 27 July 2004; received in revised form 25 September 2004; accepted 27 September 2004

**Abstract**

The potential tumor seeking MRI contrast agent $MnTPPS_4$ was labelled with the positron emitting nuclide $^{51}$Mn in no-carrier-added (n.c.a.) form. The complex formation kinetics were investigated and the apparent rate constants were determined under pseudo-first-order conditions. The derived bimolecular rate constants gave the Arrhenius parameters $E_A = 84\,\mathrm{kJ\,mol^{-1}}$ and $A = 2 \times 10^{12}\,\mathrm{s^{-1}\,M^{-1}}$. Optimum labelling conditions were derived (radiochemical yields > 99% possible, effective yields about 32%). Separation and purification of n.c.a. $^{51}MnTPPS_4$ were performed for potential human use. All impurities were < 1%.


*Keywords:* Positron emitter $^{51}$Mn; MRI contrast agents; Metallo-porphyrins; Kinetic analysis; [$^{51}$Mn]$MnTPPS_4$

## 1. Introduction

Divalent manganese next to trivalent gadolinium is the most effective base of MRI contrast agents due to its paramagnetic, i.e. proton relaxing property. Such contrast enhancers are routinely applied in patients for diagnostic purposes in medical radiology (Lauffer, 1987; Mitchell, 1997). Although free manganese ions show a higher relaxivity (Lauffer, 1987) and therefore a higher contrast in vivo when compared to their complex compounds, they have two fundamental disadvantages. Firstly, free $Mn^{2+}$ ions in the concentrations necessary for effective contrast enhancement are toxic (Kang et al., 1984; Jynge et al., 1997), and secondly, the biodistribution is an unchangeable template (cf. Kang et al., 1984; Lauffer, 1987). However, metal complexation, can reduce the toxicity and the tissue specificity can be enhanced and modulated.

To date only MnDPDP, manganese(II)-dipyridoxyl-diphosphate, Fig. 1 (Mangafodipir Trisodium™, initially synthesized by Rocklage et al., 1989), has achieved clinical importance and been tested in clinical phase III trials for detection of liver tumors. A survey of the available information was presented in a special issue of the journal Acta Radiologica (volume 38, issue 4Pt2, 1997). Wang (1998) established that tumors in

*Corresponding author. Tel.: +49 2461 613282; fax: +49 2461 612535.
*E-mail address:* s.m.qaim@fz-juelich.de (S.M. Qaim).
[1]Present address: Abteilung Nuklearmedizin, Universitätsklinikum Ulm, D-89081 Ulm, Germany.
[2]Present address: Institut für Kernchemie, Johannes Gutenberg-Universität, D-55099 Mainz, Germany.

0969-8043/$ - see front matter 
doi:10.1016/j.apradiso.2004.09.009

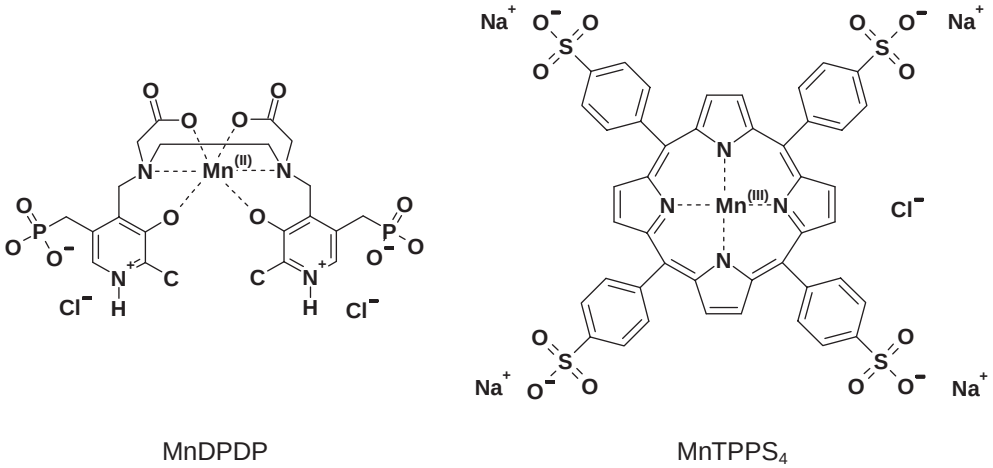


Fig. 1. Structures of MnDPDP, manganese(II)-dipyridoxyl-diphosphate (Mangafodipir Trisodium™, $MnC_{22}H_{28}N_4O_{12}P_2Cl_2$, MW = 728.3 g/mol) and $MnTPPS_4$, manganese(III)-tetraphenyl-porphin-sulfonate (Mn(III)-tetrakis(4-sulfonatophenyl)porphin, $MnC_{44}H_{24}N_4O_{12}S_4ClNa_4$, MW = 1111.3 g/mol).

the pancreas can also be imaged with the agent. Gallez et al. (1996) demonstrated that its toxicity mainly results from manganese release, despite its stability constant of $K = 10^{+15.1}\,M^{-1}$, and is attributed to the action of released $Mn^{2+}$ as a $Ca^{2+}$ antagonist (cf. Jynge et al., 1997; Brurok et al., 1999).

The manganese porphyrins represent a further class of compounds which have been examined in view of their potential as MRI contrast agents (Patronas et al., 1986; Lyon et al., 1987). Initial tests were conducted with endogenous porphyrins like protoporphyrin IX (Jackson et al., 1985) and hematoporphyrin (Bohdiewicz et al., 1990) or their derivatives (Schmiedl et al., 1993) as ligands for manganese. The most intensely studied manganese porphyrin is $MnTPPS_4$, manganese(III)-tetraphenyl-porphin-sulfonate (Mn(III)-tetrakis(4-sulfonatophenyl) porphin, Fig. 1). Koenig et al. (1987) reported its high relaxivity and Lyon et al. (1987) its extraordinary high stability in vivo. The medical interest in porphyrins is due to their tumor affinity which has been applied in boron neutron capture therapy (BNCT) (Hill et al., 1995) and in photodynamic cancer therapy (PDT) (Oleinick and Evans, 1998). Weizman et al. (2000) found that hydrophilic $TPPS_4$ localizes preferentially in the mitochondria. Although the relatively high toxicity of $TPPS_4$ ($LD_{50} = 0.5$ mmol/kg reported by Place et al., 1992) is reduced after complexation with $Mn^{III}$ (Schmiedl et al., 1992; Place et al., 1992), it has not been investigated fully. Regarding serum protein interaction, Yushmanov et al. (1996) found by in vitro experiments with excess bovine serum albumin, that $MnTPPS_4$ binds to the protein as a high-spin monomer, resulting in a significantly higher relaxivity compared to the free metalloporphyrin, well known as the PRE effect (Lauffer, 1987). The mechanism of tumor uptake and retention is evaluated controversially (Megnin et al., 1987; van Zijl et al., 1990; Fiel et al., 1993; Mäurer et al., 2000) and binding to peripheral benzodiazepine receptors has also been discussed by Bockhorst et al. (1990). Besides the tetra-sulfonated $MnTPPS_4$, the less sulfonated compounds $MnTPPS_3$ and $MnTPPS_2$ (cis and trans) were also screened by Fiel et al. (1990) regarding their relaxation properties. Although $MnTPPS_3$ showed the best tissue contrast, it was not further examined, since already $MnTPPS_4$ shows a high toxicity, its $LD_{50}$ being only by a factor of 2 higher than that of free $Mn^{2+}$ (Elizondo et al., 1991). Thus, according to Place et al. (1992), application of $MnTPPS_4$ in man as MRI contrast agent until now is not realizable, since the effective dose for sufficient contrast is only by a factor of 5 lower than the $LD_{50}$ and the skin is strongly colored brown–green by the dye. However, Els et al. (1995) observed a selective contrast enhancement in experimental brain tumors in mice. Bockhorst et al. (1993) had explained this observation by the disruption of the blood brain barrier followed by binding of the metalloporphyrin in or on tumor cells.

Since $MnTPPS_4$ has a potential to localize tumors selectively and since the available knowledge on its biodistribution is still poor, this compound was selected to demonstrate the possibility of labelling MRI relevant Mn complexes with the no-carrier-added (n.c.a.) positron emitter $^{51}Mn$ ($t_{1/2} = 46.2$ min, $I_{\beta}+ = 97\%$, $E_{\beta}+ = 2.5$ MeV). Thus, the labelled compound could allow non-invasive determination of the pharmacokinetics in man and could additionally serve as a new tumor localizing radiopharmaceutical. In contrast to the macroscopic amounts applied in MRI, bearing toxic

risks, studies with n.c.a. [$^{51}$Mn]MnTPPS$_4$ will be far safer, except for some radiation burden.

## 2. Materials and methods

### 2.1. Materials

All chemicals were of *pro analysi* (p.a.) grade. Inorganic agents such as NaOAc, $NaN_3$, and Adsorbex SAX-400 mg (anion exchanger), SCX-400 mg (cation exchanger) cartridges as well as column material LiChroprep RP-18, 25–40 μm for preparative columns were purchased from MERCK, Darmstadt, Germany. Solvents like $CH_3CN$, EtOH and acetone, as well as aqueous acids and bases like HCl or $NH_3$ were procured from Riedel-de Haën, Frankfurt, Germany. TPPS$_4$(Na$_4$) ⋯ 12 $H_2O$ (Tetraphenylporphine sulfonate or 4,4′,4″,4‴-(Porphin-5,10,15,20-tetrayl)tetrakis(benzene sulforic acid) tetrasodium dodecahydrate) and the ion exchange resins DOWEX 50 W × 8 and DOWEX 1 × 8, 200–400 mesh, were obtained in specially cleaned grade from FLUKA, Buchs, Switzerland. Isotopically enriched $^{50}$Cr (≈95%) in metallic form was purchased from EURISO-TOP, Groupe CEA, Saint-Aubin Cedex, France and CHEMOTRADE, Düsseldorf, Germany. The isotopic composition was $^{50}$Cr 94.7 ± 0.4%, $^{52}$Cr 4.84%, $^{53}$Cr 0.37%, $^{54}$Cr 0.09%; this was confirmed by ICP-MS measurements at the Central Division of Analytical Chemistry (ZCH), Forschungszentrum (FZ) Jülich, Germany. The chemical impurities (in ppm), as specified by the supplier were: Ti (< 30), Mn (< 10), Fe (< 250), Ni (< 40), Cu (80), Al (7 8 0), Si (2 0 0), and Ca (1 5 0).

For reaction mixture analysis and quality control of *MnTPPS$_4$, the reversed phase column Kromasil-5-C18, 250 × 4 mm from CS CHROMATOGRAPHIE-SERVICE, Langerwehe, Germany, was used.

Radioisotopes: *Mn represents n.c.a. radiomanganese, e.g. $^{52}$Mn ($t_{1/2}$ = 5.6 d, I($\beta^+$) = 29%, $E(\gamma_1)$ = 744.2 keV (90%)), $^{54}$Mn ($t_{1/2}$ = 312.2 d, EC = 100%, E($\gamma$) = 834.8 keV (99.98%)) or $^{51}$Mn (t1/2 = 46.2 min, $I(\beta^+)$ = 97%, $E(\gamma)$ = 749.1 keV (0.27%)). The longer-lived radiomanganese isotopes $^{52}$Mn and $^{54}$Mn were preferred for basic investigations. Pure aqueous radiotracer solutions of $^{52,54}$MnCl$_2$ and $^{51}$MnCl$_2$ were prepared at FZ Jülich as previously described (Klein et al., 2002).

Labelling experiments were conducted in Mini-Vials 20/400 (Alltech Associates Inc, Deerfield, IL, USA) with volumes up to 5 mL.

### 2.2. Instruments

For pH measurements, the pH meter CG 838 and the glass electrode type N5900A from SCHOTT, Mainz, Germany, were used. Colorimetric determination of concentrations was achieved using the UV/VIS spectrophotometer UV 160A from SHIMADZU, Japan. Quantitative $\gamma$-ray spectrometry was conducted using Ge(Li) and HPGe detectors from Canberra, Meriden, CT, USA and Ortec, Oak Ridge, TN, USA using the GammaVision_2.0 software from Ortec. Kinetic measurements were performed using the heater/stirrer type IKAMAG RTC basic controlled by the PT-100 thermo detector ETS-D4 fuzzy, both from JANKE & KUNKEL GmbH & Co KG, Staufen, Germany. For analytical HPLC, an inert (polyether–ether–ketone, PEEK) gradient system (high-pressure mixing) was used including two pumps of the type S1100 from SYKAM GmbH, Eresing, Germany. The UV/VIS detector used was S3200 from Alltech Associates Inc, Deerfield, Il, USA. The injector valve S9010 (PEEK edition) was from RHEODYNE L.P., Rohnert Park, CA, USA. The injection loop (20 μL) and the tubing were of inert peek material. The fraction collector type RediFrac was from Amersham-Biosciences AB, Uppsala, Sweden. Kinetic parameters were determined by curve fittings using the computer programme ORIGIN 3.5 (Microcal Software Inc, Northampton, MA, USA).

## 3. Experimental

### 3.1. Preparation of MnTPPS$_4$ standard

Manganese-(III)-TPPS$_4$ was prepared according to the method of Bockhorst and Hoehn-Berlage (1994), by mixing 500 μL of 1.9 mM TPPS$_4$(Na$_4$) (0.01 mmol) with 50 μL of 0.1 M $MnCl_2$ (5 mmol) solution. The mixture was heated for 20 min at 100 °C and allowed to cool at room temperature for 3 h in the presence of air.

### 3.2. UV/VIS spectra

UV/VIS spectra were recorded for both acidic and alkaline TPPS$_4$ solutions as well as for the prepared MnTPPS$_4$, and the results are shown in Fig. 2. Due to the pyrrole-*N* protonation $H_2TPPS_4 \rightarrow H_3TPPS_4 \rightarrow H_4TPPS_4$ with p$K_{3,4} \cong 4.55$ determined by Johnson et al. (1972) (cf. also p$K_3$ = 4.95 and p$K_4$ = 4.86 found for TPPS$_3$ by Itoh et al., 1975) the Soret band is shifted to longer wavelengths with the decreasing pH, i.e. with a color shift from red (alkaline) to green (acidic) as verified by Hanyz and Wrobel (2002).

### 3.3. Analysis of the reaction mixture and quality control of *MnTPPS$_4$

Optimation of the analytical separation of the chemical species present in the reaction mixture was performed using reversed phase high performance liquid

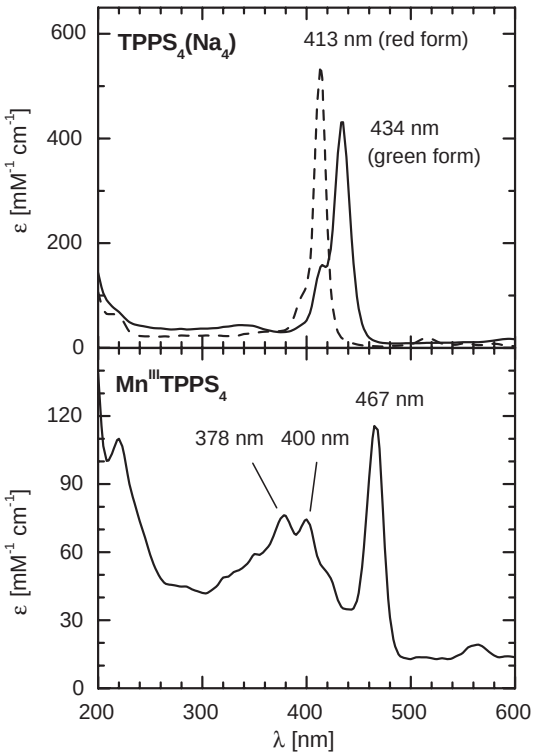


Fig. 2. Specific UV/VIS absorption spectra of $TPPS_4(Na_4)$ and $Mn^{III}TPPS_4$. Above: $TPPS_4(Na_4)$ in weakly alkaline (bordeaux red, pH 8) and acidic (light green, pH 6) medium. Specific absorption coefficients at absorption peaks ($mM^{-1}\,cm^{-1}$): 514.5 (red, 413 nm) and 426.3 (green, 434 nm). Below: $Mn^{III}TPPS_4$ (cola brown) in the presence of a 20-fold excess of $MnCl_2$. Specific absorption coefficients at absorption peaks ($mM^{-1}\,cm^{-1}$): 76.5 (378 nm), 74.2 (400 nm) and 116.0 (467 nm).

chromatography (RP-HPLC). With the RP-18 column as static phase, gradient chromatography was applied with the two partial eluents:

(A) 100 mM $NH_4Oac$ + HOAc (→pH 5) in: $CH_3CN$ : $H_2O$ = 50: 50 (v/v).
(B) 100 mM $NH_4Oac$ + HOAc (→pH 5) in: $H_2O$.

The flow rate was 1 mL/min. For optimation of HPLC separation, two test solutions were used: a bordeaux-red 38 μM $TPPS_4(Na_4)$ solution, containing 1 MBq n.c.a. $*Mn^{2+}$, and a brown 17 μM $MnTPPS_4$ solution (with molar excess of $Mn^{2+}$) which was prepared as described above and diluted. Both species, the free porphyrin and the manganese porphyrin, were detected at 434 and 467 nm, respectively, or both simultaneously at 405 nm during a chromatographic run. $*Mn^{2+}$ was detected off-line by γ-counting of the fractionized effluent.

### 3.4. Kinetic analysis

The kinetic analysis of the reaction mixture started with evaporation to dryness of 200 μL of an n.c.a. $*Mn^{2+}$ solution inside a 3 mL Mini-Vial. In a small beaker 400 μL of an aqueous, red $TPPS_4(Na_4)$ solution of defined concentration was evaporated and the cooled residue dissolved in 400 μL of aqueous HPLC eluent, consisting of 84% (B), i.e. 8% $CH_3CN$, 0.1 M $NH_4OAc$ and additional HOAc to reach the pH 5. The complete porphyrin solution was added to the reaction vial at 0 °C containing dry n.c.a. $*Mn^{2+}$ and the vial was closed by means of a cap with septum. The reaction started with the insertion of the sample into the oil bath at a defined temperature. With increasing time intervals, 30 μL aliquots were taken from the reaction mixture and quenched by addition to 10 μL of ice-cooled 0.2 M $EDTA(Na_4)$ to stop the reaction. 20 μL of this mixture was injected into the HPLC system and the effluent collected in 1.0 mL fractions. The fractions were then counted in the γ-counter.

### 3.5. Fast separation of n.c.a. $^{51}MnTPPS_4$

#### 3.5.1. Ion exchange chromatography

A mixed bed ion exchange column was prepared with a 1:1 mixture (m/m) of cation (DOWEX 50 W × 8) and anion (DOWEX 1 × 8) exchange resin; these resins are based on polystyrene as the static phase. The mesh size of both resins was 200–400, and the effective column dimensions were $d_i = 6$ mm and $h = 55$ mm. The column was conditioned with 7.7 M HCl followed by $H_2O$ washing. After addition of 200 μL of a test solution containing $TPPS_4$ and $MnTPPS_4$ (each 1 mM) onto the resin, the column was eluted first with 2 mL $H_2O$ and then with 7.7 M HCl. The effluent was fractionated and the fractions analyzed by the UV/VIS spectrometer.

#### 3.5.2. Sequential reversed phase—solid phase extraction

Preparative reversed phase (RP) columns of the same dimensions as given above were prepared using LiChroprep RP-18, 25–40 μm based on silica gel as the static phase. The eluents were prepared in a manner analogous to those used in analytical separations and were composed of the two partial eluents (A) and (B). Eluent ⟨1⟩ was prepared by mixing 16% (vol) (A) with 84% (B), thus effectively containing 8% $CH_3CN$. For an optimum separation, the evaporated crude $*MnTPPS_4$ was dissolved in 1 mL of eluent ⟨1⟩ and the resulting bordeaux-red solution loaded onto the RP column, which was previously conditioned with eluent ⟨1⟩. Flash chromatography was performed using air pressure. The elution sequence started after retention of the porphyrins within the upper 10 mm of the column. The elution sequence was: 0–7.5 min:

⟨1⟩ = 16% (A); 7.5–41 min: ⟨2⟩ = 24% (A); and 41–53 min (endless): ⟨3⟩ = 100% (A).

The separation efficiency of this procedure was verified using a synthetic mixture of the three species, *Mn, *$MnTPPS_4$ and $TPPS_4$. The mixture was prepared by adding 200 μL of an aqueous 5 mM $TPPS_4(Na_4)$ solution to 100 μL of an aqueous n.c.a. *$MnCl_2$ solution followed by evaporation within 10 min under boiling, cooling, and dissolution in 1 mL of eluent ⟨1⟩.

## 4. Results and discussion

### 4.1. Analysis of the complexation process

#### 4.1.1. Analysis of the reaction mixture and quality control of *$MnTPPS_4$

In contrast to Chengchong et al. (1994), who separated $TPPS_4$, $MnTPPS_4$ and other metalloporphyrins using ion-pair chromatography on static RP phases, we established a complete separation of the species $Mn^{2+}$, $MnTPPS_4$ and $TPPS_4$, without an ion-pair reagent in the mobile phase, using gradient elution with an eluent containing only $H_2O$, $CH_3CN$ and acetate buffer at pH 5. For optimation of chromatography several dependencies were examined, e.g. the influence of the acetonitrile content in the eluent at start or end of the gradient, as well as of the gradient slope on separation efficiency and speed; details are given elsewhere (Klein, 1998). As a final result, an optimum analytical separation was devised with the gradient sequence: 0–0.5 min: constant at 25% eluent (A); 0.5–14 min: linear gradient from 25% to 100% (A); 14–18 min: constant at 100% (A); 18–19 min: back-switching to the starting eluent with a sharp gradient. A typical analytical chromatogram is shown in Fig. 3.

#### 4.1.2. Kinetic analysis

The reaction speed of metal insertion into the central plane of porphyrins is quite low (Hambright, 1971; Johnson et al., 1972; Hambright and Chock, 1974; Smith, 1975) since—depending on the pH of the solution—first the two pyrrole protons and subsequently the whole hydrate sphere of the divalent cation has to be removed during the insertion. Therefore catalysts are used to enhance the complexation rate. A generally applicable catalyst is acetate used in the 'acetate method' (Johnson et al., 1972; Smith, 1975).

In this work, a kinetic analysis of the complexation process was conducted in order to determine the optimum complexation conditions for divalent radiomanganese with the water soluble porphyrin ligand $TPPS_4$. The kinetics at several reaction temperatures are presented in Fig. 4. They were analyzed assuming first-order kinetics, since traces of radiomanganese cations do not significantly affect the concentration of $TPPS_4$ by

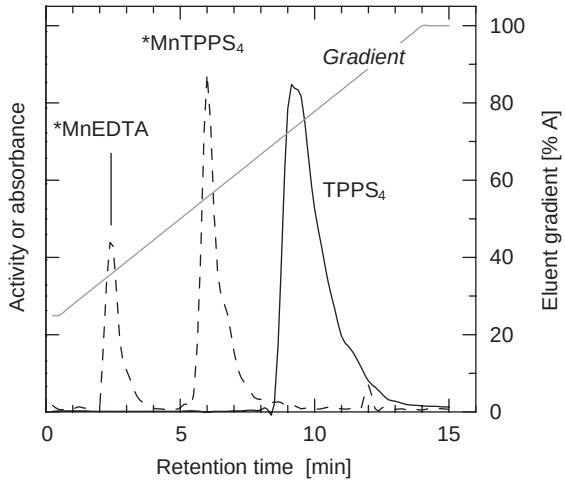


Fig. 3. Analytical separation of *$Mn^{2+}$, *$MnTPPS_4$ and $TPPS_4$ relevant to the radiochemical quality control of the radiopharmaceutical $^{51}MnTPPS_4$ applying gradient reversed phase chromatography. Separation conditions: Column: Kromasil™-5-C18, 5 μm, 250 × 4 mm; flow: 1 mL/min; eluent (A): $CH_3CN : H_2O = 50 : 50$ (v/v); eluent (B): $H_2O$; buffer content each: 100 mM $NH_4OAc + HOAc \rightarrow$ pH 5. Gradient sequence: 0 to 0.5 min: isochratic run with 25% eluent (A); 0.5 to 14 min: linear gradient 25 to 100% (A); 14 to 18 min: isochratic run at 100% (A); 18 to 19 min: back-switching to starting eluent by fast gradient. Injection volume: 20 μL. Sample: quenched (with EDTA) reaction mixture from the kinetic analysis ($T = 65\,^{\circ}C, t = 15$ min) of *MnEDTA, *$MnTPPS_4$ and $TPPS_4$.

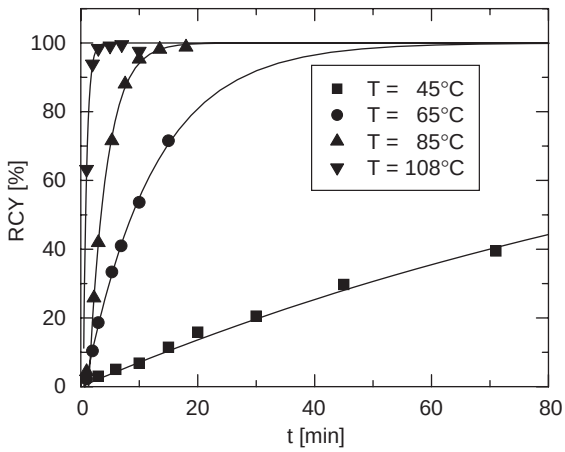


Fig. 4. Kinetics of the formation of n.c.a. *$MnTPPS_4$ by reaction of n.c.a. *$MnCl_2$ with 5 mM $TPPS_4$ in 400 μL solvent. Reaction solvent represents 84% HPLC eluent (B) and 26% (A), i.e. 8% (vol) $CH_3CN$, 0.1 M NaOAc plus HOAc→pH 5. The kinetics are presented by plotting the radiochemical yield (RCY) as a function of reaction time for four different temperatures. Mathematical fits were done by applying Eq. (1).

complexation. In practice, the function

$$\mathrm{RCY} = Y_{\max}(1 - \mathrm{e}^{-k*(t-t_0)}) \quad (1)$$

was fitted to the curves with the parameters $k$ and $Y_{\max}$, the maximum achieved yield. The radiochemical yield (RCY) represents the activity fraction of $*MnTPPS_4$ compared to the totally eluted activity from the column. Assuming an effectively bimolecular reaction between $*Mn^{2+}$ and $TPPS_4$ according to reaction scheme (2), the bimolecular rate constant $k$ resulted from the apparent constant $k*$ using the equation $k* = k[TPPS_4]_t = k[TPPS_4]_{t=0}$. The resulting rate constants $k(T)$ of second order, describing the observed net reaction

$$^{51}Mn^{2+} + (H_2)TPPS_4\{+\tfrac{1}{4}O_2\} \xrightarrow{k} [^{51}Mn^{III}TPPS_4]^+ + 2H^+\{+\tfrac{1}{2}(O^{II-})\} \quad (2)$$

are listed in Table 1. Our data are consistent with a reported value of $k = 6.79 \times 10^{-3}\,s^{-1}\,M^{-1}$ at 25 °C in acetate buffer at pH 5.4, ion strength 0.2 reported by Johnson et al. (1972). In Eq. (2) it is assumed, that the oxidation of $Mn^{II}$ to $Mn^{III}$ by oxygen is very fast and thus irrelevant for the rate constant $k$ (Boucher, 1972). The Arrhenius equation parameters (Wilkins, 1991), activation energy $E_A$ and collision factor $A$, were derived from the $k(T)$ data pairs shown in Fig. 5. Two mathematical fits were applied through the four data points, an un-weighted and an error-weighted one. The resulting values for $E_A$ and $A$ are $86.1 \pm 2.7\,kJ\,mol^{-1}$ and $(4.1 \pm 3.7) \times 10^{12}\,s^{-1}\,M^{-1}$ from the un-weighted fit and $82.1 \pm 2.4\,kJ\,mol^{-1}$ and $(1.1 \pm 0.7)\ 10^{12}\,s^{-1}\,M^{-1}$ for the error-weighted fit, respectively.

Despite the relatively small visual difference between the two fit functions, the difference in the two collision factors is significant, which is consistent with their respective high errors in the range of 80%. The activation energies, however, differ less and are comparable to the literature value of 78.24 kJ/mol for the manganese(II) insertion into tetrapyridylporphine TPPy

Table 1
Effective observed rate constants k for the assumed bimolecular reaction between $Mn^{2+}$ and $(H_2)TPPS_4$ (cf. Eq. (2)) in 400 μL solvent[a] in the presence of oxygen (air) at four different temperatures

| T (°C) | $k$ ($s^{-1}\,M^{-1}$) |
|---|---|
| 44 ± 2 | 0.0244 ± 0.0024 |
| 65 ± 2 | 0.286 ± 0.029 |
| 85 ± 2 | 1.10 ± 0.11 |
| 108 ± 2 | 5.9 ± 0.7 |

[a]Solvent contains 5 mM $TPPS_4$ , 84% HPLC eluent (B), rest (A), i.e. 8% (vol) $CH_3CN$, 0.1 M NaOAc plus HOAc → pH 5.

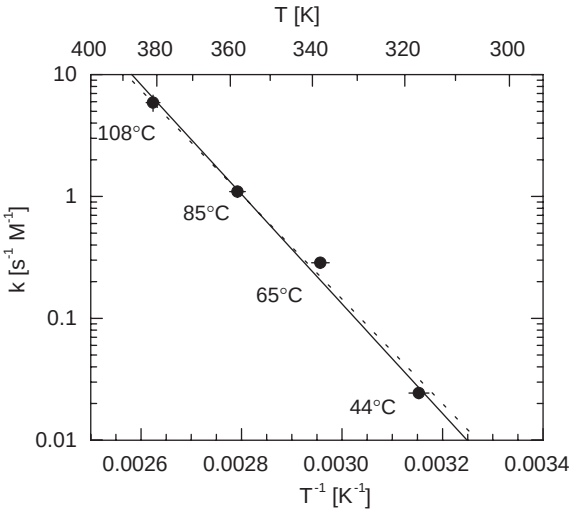


Fig. 5. Determination of the Arrhenius parameters *activation energy* ($E_A$) and *collision factor* (A) for the seemingly bimolecular reaction between $Mn^{2+}$ and porphyrin $TPPS_4$ (cf. Eq. (2)) by plotting the observed rate constants $k$ (log scale) against reciprocal absolute temperature $T$. Two mathematical fits of the Arrhenius equation through the experimental data are shown: error-weighted (solid line) and error-unweighted (dashed line) fit.

reported by Boucher (1972). The complexation reaction in reality, however, is not simply bimolecular as assumed in the chemical Eq. (2), but more complex. Formally, it involves at least a two-step-process (Boucher, 1972):

$$^{51}Mn^{2+} + (H_2)TPPS_4 \underset{k_{-1}}{\overset{k_1}{\longleftrightarrow}} {}^{51}Mn^{II}TPPS_4 + 2H^+, \quad (3)$$

$$^{51}Mn^{II}TPPS_4 + \tfrac{1}{4}O_2 \xrightarrow{k_2} [^{51}Mn^{III}TPPS_4]^+ + \tfrac{1}{2}(O^{II-}). \quad (4)$$

The first step is probably rate determining ($k_2 > k_1$), while the second one may be fast and irreversible, as expressed by Eq. (4). However, since no metalloporphyrin formation is observed in the absence of $O_2$ (Boucher, 1972), it is obvious that $k_{-1} \gg k_1$. The above equations also reveal that the net kinetics should not depend only on the concentration of the porphyrin $(H_2)TPPS_4$, but also on the pH and the oxygen concentration of the reaction solution. Attempts were made to verify the Arrhenius parameters $E_A$ and $A$ by examination of the influence of the porphyrin concentration on the radiochemical yield for a constant reaction time according to formula (5) which is analogous to (1),

$$\mathrm{RCY} = Y_{\max}(1 - e^{-k**[TPPS_4]}) \quad (5)$$

with $k^{**} = k \times t$.

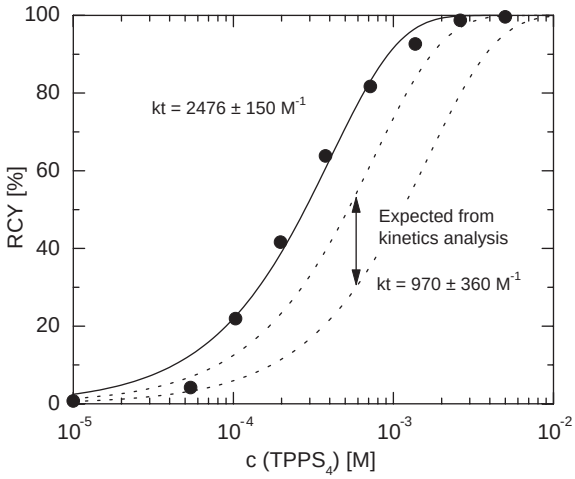


Fig. 6. Dependence of the radiochemical yield of $*MnTPPS_4$ on ligand $TPPS_4$ concentration. Experimental data points are results obtained using reaction volume 200 μL. The solid curve fit was done based on Eq. (5). The dashed curves describe expected ligand dependence, calculated from kinetic analyses with reaction volumes of 400 μL.

The results are shown in Fig. 6. The experimental data are fitted well by Eq. (5), thus verifying the partial reaction for radiomanganese as first order. However, the apparent rate constant $k^{**}$ was about a factor of 2 higher than expected from the data of the previous kinetic analysis. The only difference of this experiment compared to the kinetic ones was the reduction of the reaction volume from 400 to 200 μL. Obviously the participating oxidation reaction (4) is not as fast as expected, i.e. $k_2$ is not much larger than $k_1$, resulting in an enhanced kinetic importance of the oxidation step. In view of the low physical solubility of $O_2$ in the hot reaction mixture, possibly the ratio of liquid surface to liquid volume is relevant. Thus, the observable net kinetics may strongly depend on the geometry of the reaction vial and of the reaction volume.

The optimum reaction parameters for the experimental setup can now be calculated, if the kinetic formula for the radiochemical yield—Eq. (1)—with all parameters substituted by their respective formulas is transformed into the form:

$$\text{temperature} = \text{function}\ ([\text{TPPS4}],\ t,\ Y_{\text{net}}).$$

$Y_{\text{net}}$ represents the effective net yield of $^{51}MnTPPS_4$ at the time $t$ including losses by radioactive decay. For a chosen reaction time t and a desired net yield $Y_{\text{net}}$, the temperature $T$ can be plotted as a function of $TPPS_4$ concentration, resulting in a hyperbolic function. The result of the optimation efforts is finally the achievement of the highest effective net activity yield ($Y_{\text{net}} > 90\%$) at the lowest possible precursor concentration, thus easing the preparative purification of the n.c.a. product. However, the educt concentration cannot be simply reduced to any value, because otherwise correspondingly increasing reaction temperatures would have to be applied due to the hyperbolic shape of the curve. At high temperatures undesired chemical disintegrations might occur, which would lower $Y_{\text{net}}$ and cause additional separation problems during the purification process.

Thus, at least a temperature of 127 °C (400 K) must be chosen, if after $t = 5$ min a radiochemical yield of 99.9%—i.e. an effective net yield of 92.7% in $^{51}MnTPPS_4$–is to be reached, starting with n.c.a. $^{51}Mn^{2+}$ and 1 mM $TPPS_4$ in 400 μL HPLC eluent (8% $CH_3CN$, 0.1 M $NH_4OAc$ plus HOAc → pH 5) inside a sealed 2 mL Mini-Vial.

### 4.2. Fast separation of n.c.a. $^{51}MnTPPS_4$

After the synthesis of n.c.a. $^{51}MnTPPS_4$, a rapid and efficient separation of the product from macroscopic amounts of the precursor $TPPS_4$ as well as from possibly excessive $^{51}Mn^{2+}$ ions is necessary.

First separation attempts of the species $*Mn^{2+}$, $TPPS_4$ and $*MnTPPS_4$ on a preparative scale were made using the self-prepared mixed-bed ion-exchanger based on a polystyrene core. Although $*Mn^{2+}$ was elutable the porphyrins could not be eluted, even with high ion strength and organic additive. Obviously, a synergy of ion binding and apolar van der Waals binding causes an extremely strong porphyrin retention. Switching to a cation-exchange cartridge (SCX, sodium form) with silica core resulted in the retention of $*Mn^{2+}$ during the elution with $H_2O$, while both $*MnTPPS_4$ and $TPPS_4$ were eluted quickly. Thus, not only the free porphyrin, but also the manganese porphyrin was present in neutral or anionic form. When the respective anion exchange cartridge (SAX, chloride form) was used, $*Mn^{2+}$ was not retained, while the porphyrins remained fixed. The use of hydrochloric acid as eluent did not result in a sufficient baseline separation between $TPPS_4$ and the following $*MnTPPS_4$. Nevertheless, this elution sequence indicates that the $MnTPPS_4$ is more strongly negatively charged than the free porphyrin, probably due to axial anionic ligands such as chloride.

Finally a separation method was devised, making use of the analytical HPLC separation of the three relevant species. An optimum sequence was found as described in the experimental section. The respective elution profile is shown in Fig. 7. The major advantage of this sequential solid phase extraction is the large distance, over which the species are eluted subsequently. Thus, the product $*MnTPPS_4$ can be selectively eluted with a high chemical and radiochemical purity after separation of free $*Mn^{2+}$ with an almost aqueous eluent. The small radioactive peak ("?") behind the bulk elution of

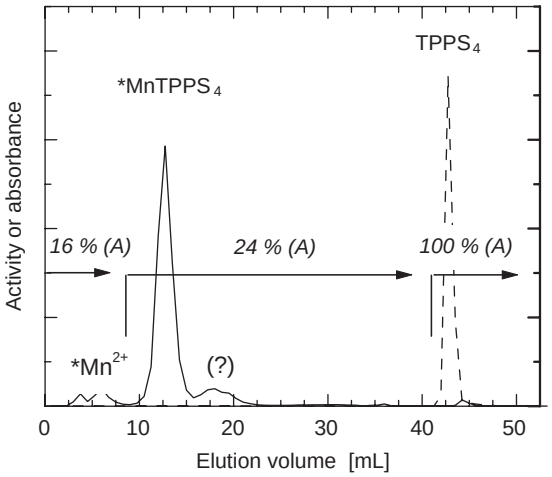


Fig. 7. Purification of the radiopharmaceutical $^{51}MnTPPS_4$ on a preparative scale using a reversed phase (LiChroprep$^{TM}$) and subsequent solid phase extraction (SPE). Column filling: $d_i = 6\,mm, h = 55\,mm$; for elution sequences see experimental section (partial eluent (A): $CH_3CN : H_2O = 50 : 50$ (v/v); eluent (B): $H_2O$; buffer content each: 100 mM $NH_4OAc + HOAc \rightarrow pH\ 5$). Elution chart: $^{51}Mn^{2+}$, $^{51}MnTPPS_4$, $TPPS_4$.

*$MnTPPS_4$ probably corresponds to the metalloporphyrin at another protonation level (cf. the four sulfonato groups). Thus, the product can be separated quantitatively (>99.5%) within a 13 mL fraction, or the main fraction (~80%) within only 6 mL. The remaining product impurities are <1% *$Mn^{2+}$ and $TPPS_4$. Together with the $Mn^{2+}$ fraction polar impurities of the commercially available $TPPS_4(Na_4)$ (Bockhorst and Hoehn-Berlage, 1994) are also eluted, as UV/VIS analyses of the fractionized effluent revealed. The collected product fraction of 13 mL is further passed through a cation exchange cartridge (SCX) in $H^+$ form, to extract $NH_4^+$ from the buffered reaction solvent (and any *$Mn^{2+}$ still present). The solution is then evaporated to dryness and dissolved in 0.10 M NaCl, containing 0.05 M phosphate buffer at pH 7.

After sterile filtration and in the case of the positron emitter $^{51}Mn$, the final solution of $^{51}MnTPPS_4$ is ready for test injections into animals or humans. Alternatively, if desired, the evaporated $^{51}MnTPPS_4$ residue can be dissolved in an isotonic and buffered solution containing macroscopic amounts of non-radioactive $MnTPPS_4$ in order to study pharmacokinetics of the contrast agent in suitable animals under common MRI conditions by means of PET. In this context it would be of interest, whether a difference is observed in pharmacokinetics with and without macroscopic carrier. The labelling of the porphyrin $TPPS_4$ with $^{51}Mn$, as well as the chromatographic purification of n.c.a. $^{51}MnTPPS_4$ can be conducted directly after the production of n.c.a. $^{51}Mn$ (Klein et al., 2002) in a remotely controlled process unit (cf. Klein, 1998).

## 5. Conclusion

The radiopharmaceutical metalloporphyrin $^{51}MnTPPS_4$ can be obtained in an overall effective yield of about 32% (decay considered, 20% overall nuclide losses assumed), provided the optimum labelling parameters are chosen: 30 min for the automated production of $^{51}Mn^{2+}$, another 30 min for automated labelling and purification of the radiopharmaceutical and with a 99.9% RCY for the labelling step.

Some attempts have been made to introduce porphyrins as diagnostic tumor probes in nuclear medicine(Lavallee and Fawwaz, 1986; Crone-Escanye et al., 1988; Ali et al., 1997). Moreover, Schomäcker et al. (1999) tried to introduce porphyrins into endoradiotherapy. However, little scientific resonance followed and thus the potential of porphyrins to address tumors in nuclear medicine rather than in MRI is still underestimated.

## Acknowledgements

We are grateful to the operators of the cyclotron CV 28 for many irradiations and to M. Jelinski for assistance.

## References

Ali, S.A., Cesani, F., Nusynowitz, M.L., Briscoe, E.G., Shirtliff, M.E., Mader, J.T., 1997. Skeletal scintigraphy with technetium-99m-tetraphenyl porphyrin sulfonate for the detection and determination of osteomyelitis in an animal model. J. Nucl. Med. 38 (12), 1999–2002.

Bockhorst, K., Hoehn-Berlage, M., 1994. An optimized synthesis of manganese meso-tetra(4-sulfonatophenyl)porphine: a tumor selective MRI contrast agent. Tetrahedron 50, 8657–8660.

Bockhorst, K., Hoehn-Berlage, M., Kocher, M., Hossmann, K.-A., 1990. Proton relaxation enhancement in experimental brain tumors—in vivo NMR study of manganese(III)TPPS in rat brain gliomas. Magn. Reson. Imaging 8, 499–504.

Bockhorst, K., Hoehn-Berlage, M., Ernestus, R.I., Tolxdorff, T., Hossmann, K.A., 1993. NMR contrast enhancement of experimental brain tumors with MnTPPS: quantitative evaluation by in vivo relaxometry. Magn. Reson. Imaging 11, 655–663.

Bohdiewicz, P.J., Lavallee, D.K., Fawwaz, R.A., Newhouse, J.H., Oluwole, S.F., Alderson, P.O., 1990. Mn(III) hematoporphyrin, a potential MR contrast agent. Invest. Radiol. 25, 765–770.

Boucher, L.J., 1972. Manganese porphyrin complexes. Coord. Chem. Rev. 7, 289–329.

Brurok, H., Berg, K., Sneen, L., Grant, D., Karlsson, J.O.G., Jynge, P., 1999. Cardiac metal contents after infusions of manganese. An experimental evaluation in the isolated Rat Heart. Invest. Radiol. 34, 470–476.

Chengchong, L., Fulong, T., Lihong, W., Miaorong, T., 1994. Separation of trace copper, cobalt, manganese and zinc by ion-pair high-performance liquid chromatography and their spectrophotometric determination. Fenxi Huaxue (Chin. J. Anal. Chem.) 22, 552–555 (in Chinese).

Crone-Escanye, M.C., Anghileri, L.J., Robert, J., 1988. In vivo distribution of Mn-54-hematoporphyrin derivative in tumor bearing mice. J. Nucl. Med. Allied Sci. 32, 237–241.

Elizondo, G., Fretz, C.J., Stark, D.D., Rocklage, S.M., Quay, S.C., Worrah, D., Tsang, Y.-M., Chen, M.C.-M., Ferrucci, J.T., 1991. Preclinical Evaluation of MnDPDP: new paramagnetic hepatobiliary contrast agent for MR imaging. Radiology 178, 73–78.

Els, T., Eis, M., Hoehn-Berlage, M., Hossmann, K.-A., 1995. Diffusion weighted MR imaging of experimental brain tumors in rats. Magma 3, 13–20.

Fiel, R.J., Musser, D.A., Mark, E.H., Mazurchuk, R., Alletto, J.J., 1990. A comparative study of manganese meso-sulfonatophenyl porphyrins: contrast enhancing agents for tumors. Magn. Reson. Imaging 8, 255–259.

Fiel, R., Mark, E., Button, T., Gilani, S., Musser, D., Cohen, J.S., Place, D.A., Faustino, P.J., 1993. Tumor-selective contrast enhancing agent Mn(III) meso-[tri(4-sulfonatophenyl)phenyl]porphine ($MnTPPS_3$). Magn. Reson. Imaging 11, 1079–1081.

Gallez, B., Bacic, G., Swartz, H.M., 1996. Evidence for the dissociation of the hepatobiliary MRI contrast agent Mn-DPDP. Magn. Reson. Med. 35, 14–19.

Hambright, P., 1971. The coordination chemistry of metalloporphyrins. Coord. Chem. Rev. 6, 247–269.

Hambright, P., Chock, P.B., 1974. Metal-porphyrin interactions. III. A dissociative-interchange mechanism for metal ion incorporation into porphyrin molecules. J. Am. Chem. Soc. 96, 3123–3131.

Hanyz, I., Wrobel, D., 2002. The influence of pH on charged porphyrins studied by fluorescence and photoacoustic spectroscopy. Photochem. Photobiol. Sci. 1 (2), 126–132.

Hill, J.S., Kahl, S.B., Stylli, S.S., Nakamura, Y., Koo, M.S., Kaye, A.H., 1995. Selective tumor kill of cerebral glioma by photodynamic therapy using boronated porphyrin photosensitizer. Proc. Natl. Acad. Sci. USA 92, 12126–12130.

Itoh, J.I., Yotsuyanagi, T., Aomura, K., 1975. Spectrophotometric determination of copper with a,b,g,d-tetraphenylporphine trisulfonate. Anal. Chim. Acta 74, 53–60.

Jackson, L.S., Nelson, J.A., Case, T.A., Burnham, B.F., 1985. Manganese protoporphyrin IX, A potential intravenous paramagnetic NMR contrast agent: preliminary communication. Invest. Radiol. 20 (5), 226–229.

Johnson, N., Khosropour, R., Hambright, P., 1972. Kinetics of the acetate catalyzed insertion of copper into a diacid porphyrin. Inorg. Nucl. Chem. Lett. 8, 1063–1067.

Jynge, P., Brurok, H., Asplund, A., Towart, R., Refsum, H., Karlsson, J.O.G., 1997. Cardiovacular safety of MnDPDP and $MnCl_2$. Acta Radiol. 38, 740–749.

Kang, Y.S., Gore, J.C., Armitage, I.M., 1984. Studies of factors affecting the design of NMR contrast agents: manganese in blood as a model system. Magn. Reson. Med. 1, 396–409.

Klein, A.T.J., Rösch, F., Coenen, H.H., Qaim, S.M., 2002. Production of the positron emitter $^{51}Mn$ via the $^{50}Cr(d,n)$ reaction: targetry and separation of no-carrier-added radiomanganese. Radiochim. Acta 90, 167–177.

Klein, A., 1998. Produktion von n.c.a. $^{51}Mn$ zur in vivo PET-Evaluierung von Kontrastmitteln für die Magnetresonanztomographie (MRT). Report Juel-3553, Jülich, Germany.

Koenig, S.H., Brown III, R.D., Spiller, M., 1987. The anomalous relaxivity of $Mn^{3+}(TPPS_4)$. Magn. Reson. Med. 4, 252–260.

Lauffer, R.B., 1987. Paramagnetic metal complexes as water proton relaxation agents for NMR imaging: therory and design. Chem. Rev. 87, 901–927.

Lavallee, D.K., Fawwaz, R., 1986. The synthesis and characterization of $^{111}In$ hematoporphyrin derivative. Nucl. Med. Biol. 13 (6), 639–641.

Lyon, R.C., Faustino, P.J., Cohen, J.S., Katz, A., Mornex, F., Colcher, D., Baglin, C., Koenig, S.H., 1987. Tissue distribution and stability of metalloporphyrin MRI contrast agents. Magn. Reson. Med. 4, 24–33.

Mäurer, J., Strauss, A., Ebert, W., Bauer, H., Felix, R., 2000. Contrast-enhanced high resolution magnetic resonance imaging of pigmented malignant melanoma using Mn-$TPPS_4$ and Gd-DTPA: experimental results. Melanoma Res. 10 (1), 40–46.

Megnin, F., Faustino, P.J., Lyon, R.C., Lelkes, P.I., Cohen, J.S., 1987. Studies on the mechanism of selective retention of porphyrins and metalloporphyrins by cancer cells. Biochim. Biophys. Acta 929, 173–181.

Mitchell, D.G., 1997. MR imaging contrast agents—what's in a name? J. Magn. Reson. Imaging 7 (1), 1–4.

Oleinick, N.L., Evans, H.H., 1998. The photobiology of photodynamic therapy: cellular targets and mechanisms. Radiat. Res. 150, S146.

Patronas, N.J., Cohen, J.S., Knop, R.H., Dwyer, A.J., Colcher, D., Lundy, J., Mortex, F., Hambright, P., Son, M., Myers, C.E., 1986. Metalloporphyrin contrast agents for magnetic resonance imaging of human tumors in mice. Cancer Treatm. Rep. 70, 391–395.

Place, D.A., Faustino, P.J., Berghmanns, K.K., Van Zijl, P.C.M., Chesnick, A.S., Cohen, J.S., 1992. MRI contrast-dose relationship of manganese (III) tetra(4-sulfonatophenyl)porphin with human xenograft tumors in nude mice at 2.0 T. Magn. Reson. Imaging 10, 919–928.

Rocklage, S.M., Cacheris, W.P., Quay, S.C., Hahn, F.E., Raymond, K.N., 1989. Manganese(II) N,N′-dipyridoxylethylenediamine-N,N′-diacetate 5,5′-bis(phosphate). Synthesis and characterization of a paramagnetic chelate for magnetic resonance imaging enhancement. Inorg. Chem. 28, 477–485.

Schmiedl, U.P., Nelson, J.A., Starr, F.L., Schmidt, R., 1992. Hepatic contrast-enhancing properties of manganese-mesoporphyrin and manganese-TPPS4. A comparative magnetic resonance study in rats. Invest. Radiol. 27, 536–542.

Schmiedl, U.P., Nelson, J.A., Robinson, D.H., Michalson, A., Starr, F., Frenzel, T., Ebert, W., Schumann-Giamieri, G., 1993. Pharmaceutical properties; biodistribution; and imaging characteristics of manganese-mesoporphyrin; a potential hepatobiliary contrast agent for magnetic resonance imaging. Invest. Radiol. 28, 925–932.

Schomäcker, K., Gaidouk, M.I., Rumyantseva, V.D., Fischer, T., Lohr, H., Salditt, S., Liebenhoff, S., Schicha, H., 1999.

Synthese tumoraffiner Yb-169- und Y-90-Porphyrin-Komplexe und tierexperimentelle Untersuchung verschiedener Yb-169-Porphyrine. Nuklearmedizin 38 (7), 285–291.

Smith, K.M. (Ed.), 1975, Porphyrins and metalloporphyrins. Elsevier Publishers, Amsterdam, NL.

Wang, C., 1998. Mangafodipir trisodium (MnDPDP)-enhanced magnetic resonance imaging of the liver and pancreas. Acta Radiol. Suppl. 415, 1–31.

Weizman, E., Rothmann, C., Greenbaum, L., Shainberg, A., Adamek, M., Ehrenberg, B., Malik, Z., 2000. Mitochondrial localization and photodamage during photodynamic therapy with tetraphenylporphines. J. Photochem. Photobiol. B. 59 (1-3), 92–102.

Wilkins, R.G., 1991. Kinetics and mechanism of reactions of transition metal complexes. VCH Publishers, Weinheim, Germany.

Yushmanov, V.E., Tominaga, T.T., Borissevitch, I.E., Imasato, H., Tabak, M., 1996. Binding of manganese and iron tetraphenylporphine sulfonates to albumin is relevant to their contrast properties. Magn. Reson. Imaging 14, 255–261.

Van Zijl, P.C.M., Place, D.A., Cohen, J.S., Faustino, P.J., Lyon, R.C., Patronas, N.J., 1990. Metalloporphyrin magnetic resonance contrast agents. Feasibility of tumor-specific magnetic resonance imaging. Acta Radiol. Suppl. S 374, 75–79.